
Neural Topographic Factor Analysis for fMRI Data

Eli Z. Sennesh

Khoury College of Computer Sciences
Northeastern University
Boston, MA 02115
esennesh@kccis.neu.edu

Zulqarnain Khan

Department of Electrical Engineering
Northeastern University
khanzu@ece.neu.edu

Jennifer Dy

Department of Electrical Engineering
Northeastern University
jdy@ece.neu.edu

Ajay B. Satpute

Department of Psychology
Northeastern University
a.satpute@northeastern.edu

J. Benjamin Hutchinson

Department of Psychology
University of Oregon
bhutch@uoregon.edu

Jan-Willem van de Meent

Khoury College of Computer Sciences
Northeastern University
j.vandemeent@northeastern.edu

Abstract

Neuroimaging experiments produce a large volume (gigabytes) of high-dimensional spatio-temporal data for a small number of sampled participants and stimuli. Analyses of this data commonly compute averages over all trials, ignoring variation within groups of participants and stimuli. To enable the analysis of fMRI data without this implicit assumption of uniformity, we propose Neural Topographic Factor Analysis (NTFA), a deep generative model that parameterizes factors as functions of embeddings for participants and stimuli. We evaluate NTFA on a synthetically generated dataset as well as on three datasets from fMRI experiments. Our results demonstrate that NTFA yields more accurate reconstructions than a state-of-the-art method with fewer parameters. Moreover, learned embeddings uncover latent categories of participants and stimuli, which suggests that NTFA takes a first step towards reasoning about individual variation in fMRI experiments.

1 Introduction

Analyzing neuroimaging studies is both a large data problem and a small data problem. A single scanning run typically involves hundreds of full-brain scans that each contain tens of thousands of spatial locations (to which we refer as voxels). At the same time, neuroimaging studies tend to have limited statistical power. A typical study considers a cohort of 20-50 participants undergoing tens of stimuli (or even fewer). A challenge in this domain is to develop analysis methods that can appropriately account for both the commonalities and variations among participants and stimulus effects, while also scaling to tens of gigabytes of data and providing a means to reason about the confidence level of predictions.

In this paper, we develop Neural Topographic Factor Analysis (NTFA)¹, a family of models for analysis of spatio-temporal fMRI data suitable for reasoning about variations among differing participants and stimuli. NTFA extends Topographic Factor Analysis (TFA), an established technique

¹Source code submitted with paper and available on Github by request.

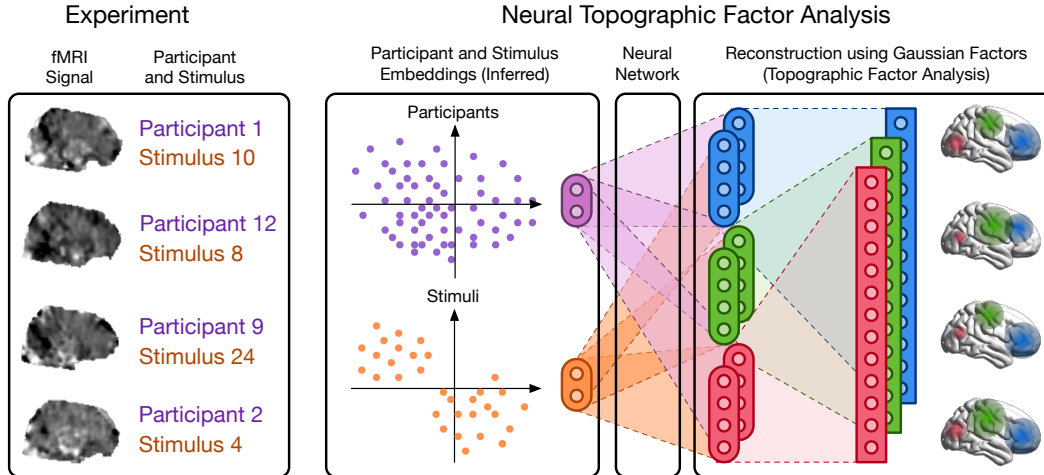


Figure 1: **Overview of Neural Topographic Factor Analysis (NTFA)**: We extend topographic factor analysis (TFA) [Manning et al., 2014b,a] to decompose the fMRI signal into distinct factors (shown in red, green and blue in the figure) that correspond to spatially and temporally related brain activity across individuals. We represent subjects (purple) and stimuli (orange) with embedding vectors, which together define the distribution on the factor parameters for each trial.

for fMRI analysis [Manning et al., 2014b], with a deep generative prior. This prior defines a distribution over embeddings (i.e. vectors of features) for each participant and stimulus, along with a conditional distribution over spatial and temporal factors, which is parameterized by a simple neural network. The result is a structured deep probabilistic model that can characterize variation among participants and stimuli, as well as interaction effects between the two.

We evaluate NTFA on four datasets. We validate that inference and learning recover known group structure in a synthetic dataset, simulated from a simplified generative model that has been designed to contain distinguishable clusters of participants and stimuli. We additionally consider two datasets from publicly available fMRI studies. In the first, participants listen to the narrative “Pie Man” [Simony et al., 2016]. In the second, participants with and without major depressive disorder listen to audio stimuli and music [Lepping et al., 2016]. Finally, we report results from a pilot study on the neural basis of fear that capitalized on the utility of our NTFA model. Participants were shown video clips of spiders, looming heights, and threatening social situations that varied in how much fear they evoked both within category (i.e. there were both low and high fear inducing spider videos), and across individuals (i.e. some participants were, on average, more and some less influenced by the videos). Our NTFA model, which was naive to the stimulus category and individual differences in fear experience, nevertheless recovered meaningful subject and stimulus embeddings in a fully unsupervised manner. The stimulus embeddings recovered the stimulus categories of videos, and the participant embeddings correlated with behavioral measures of fear sensitivity.

The main contributions of this paper are:

- We develop NTFA (Section 3), a new model for analysis of fMRI data that infers embeddings for participants and stimuli which are shared across experiment trials. NTFA can be trained using an accompanying method for black-box variational inference [Ranganath et al., 2014].
- We evaluate NTFA on four datasets (Section 4) and find that NTFA achieves a higher log-likelihood than Hierarchical Topographic Factor Analysis (HTFA) [Manning et al., 2014a, 2018], which is representative of the state of the art (Section 4.2).
- We demonstrate that embeddings, inferred in a fully unsupervised manner, correlate with experimental design variables and behavioral measures (Section 4.2). To our knowledge, NTFA is the first model that is able to characterize participants and stimuli in this manner.

Figure 1 shows an overview of the proposed approach. Section 2 covers the related work in Factor Analysis for neuroimaging data, primarily HTFA which forms the basis for this work. Section 3 develops the NTFA model and Section 4 discusses experiments and results.

2 Topographic Factor Analysis Methods for fMRI Data

Factor analysis methods are widely used to reduce the dimensionality of neuroimaging data, while at the same time capturing meaningful regularities. These methods decompose the fMRI signal for a trial $Y \in \mathbb{R}^{T \times V}$ with T time points and V voxels into a product $Y \simeq W \cdot F$ between a lower-rank matrix of weights $W \in \mathbb{R}^{T \times K}$ and a lower-rank matrix of factors $F \in \mathbb{R}^{K \times V}$, where typically $K \ll V$. General-purpose methods that have been applied to fMRI data include Principal Component Analysis (PCA) [Abdi and Williams, 2010] and Independent Component Analysis (ICA) [Hyvärinen et al., 2001]. A number of methods have also been developed specifically for fMRI analysis, such as Hyper-Alignment (HA) [Haxby et al., 2011] and Topographic Latent Source Analysis (TLSA) [Gershman et al., 2011].

In this paper, we extend topographic factor analysis [Manning et al., 2014b] and Hierarchical Topographic Factor Analysis [Manning et al., 2014a, 2018]. TFA is a probabilistic factor analysis model that uses radial basis functions to define spatially smooth factors. HTFA itself extends TFA by assuming that model parameters are drawn from a hierarchical Gaussian prior shared across trials.

Concretely, let us consider a dataset comprising N trials (i.e. continuous recordings) each of which contain T time points for voxels at V spatial positions. TFA defines a probabilistic model that approximates each trial $Y_n \simeq W_n F_n$ as a product between a matrix of K time-varying weights $W_n \in \mathbb{R}^{T \times K}$ and a matrix $F_n \in \mathbb{R}^{K \times V}$ of K spatially-varying factors. To do so, TFA assumes that the data is noisily sampled from the inner product of the weights and factors matrices

$$Y_n \sim \mathcal{N}(W_n \cdot F_n, \sigma^Y). \quad (1)$$

TFA combines this likelihood $p(Y_n | W_n, F_n)$ with a prior $p(W_n, F_n)$, which defines a probabilistic model $p(Y_n, W_n, F_n)$. TFA performs inference by approximating the posterior $p(W_n, F_n | Y_n)$ with a variational distribution $q(F_n, W_n | \lambda)$, and optimizing its parameters.

TFA assumes means $\mu_{n,k}^W$ and standard deviations $\sigma_{n,k}^W$ for each factor's weights over time, and defines a hierarchical Gaussian prior of the form

$$W_{n,t,k} \sim \mathcal{N}(\mu_{n,k}^W, \sigma_{n,k}^W), \quad \mu_{n,k}^W \sim p(\mu^W), \quad \sigma_{n,k}^W \sim p(\sigma^W).$$

To model the factors F_n , TFA employs a kernel function that ensures spatial smoothness of factor values $F_{n,k,v}$ at similar voxel positions $x_v^G \in \mathbb{R}^3$. This kernel function κ is normally a radial basis function (RBF), which models each factor $k \in K$ as a Gaussian with center at a spatial location $x_{n,k}^F \in \mathbb{R}^3$, whose width is determined by the kernel hyper-parameters $\rho_{n,k}^F$,

$$F_{n,k,v} = \kappa(x_v^G, x_{n,k}^F; \rho_{n,k}^F), \quad (2)$$

with Gaussian priors over both the positions and widths,

$$x_{n,k}^F \sim p(x^F), \quad \rho_{n,k}^F \sim p(\rho^F). \quad (3)$$

Interpreting factor analysis probabilistically enables us to incorporate additional assumptions in order to capture variation and similarities between multiple sets of trials. HTFA [Manning et al., 2014a, 2018], introduces variables \bar{x}_k^F and $\bar{\rho}_k^F$ representing each factor's mean positions and widths across trials,

$$x_{n,k}^F \sim p(x_{n,k}^F | \bar{x}_k^F), \quad \bar{x}_k^F \sim p(\bar{x}^F), \quad (4)$$

$$\rho_{n,k}^F \sim p(\rho_{n,k}^F | \bar{\rho}_k^F), \quad \bar{\rho}_k^F \sim p(\bar{\rho}^F). \quad (5)$$

This prior is able to model multimodal responses to an extent, in the sense that factor positions and widths for individual trials are allowed to vary relative to a shared mean. However, the Gaussian hyperprior in HTFA assumes that neural responses across trials ought to have a unimodal distribution.

3 Neural Topographic Factor Analysis

NTFA extends TFA to model the range of variation across participants and stimuli. We assume exactly the same factor analysis model as TFA, which is to say that we model the fMRI signal as a linear combination of time-dependent weights and spatially varying Gaussian factors. NTFA additionally infers *embedding vectors* for individual participants and stimuli. We then learn a mapping from embeddings to the parameters of the likelihood model, parameterized by a neural network. This replaces the unimodal Gaussian hyperprior in HTFA with a deep generative model, and incorporates a mechanism for parameter sharing across trials.

We model trials $n \in \{1, \dots, N\}$ in which participants $p_n \in \{1, \dots, P\}$ undergo a set of stimuli $s_n \in \{1, \dots, S\}$ and are scanned for T time points. We assume that participant embeddings $\{z_1^p, \dots, z_p^p\}$ and stimulus embeddings $\{z_1^s, \dots, z_s^s\}$ are shared across trials. For simplicity, we will assume that both embeddings have the same dimensionality D and are distributed according to a Gaussian prior

$$z_p^p \sim \mathcal{N}(0, I), \quad z_s^s \sim \mathcal{N}(0, I). \quad (6)$$

For each participant p , we define the RBF center x_p^F and log-width ρ_p^F in terms of a neural mapping

$$x_p^F \sim \mathcal{N}(\mu_p^x, \sigma_p^x), \quad \mu_p^x, \sigma_p^x \leftarrow \eta_{\theta}^{F,x}(z_p^p), \quad (7)$$

$$\rho_p^F \sim \mathcal{N}(\mu_p^{\rho}, \sigma_p^{\rho}), \quad \mu_p^{\rho}, \sigma_p^{\rho} \leftarrow \eta_{\theta}^{F,\rho}(z_p^p). \quad (8)$$

Here η_{θ}^F is a neural network parameterized by a set of weights θ , which models how variations between participants and stimuli affect the factor positions and widths in brain activations. We similarly assume that a neural network parameterizes the distribution over weights $W_{n,t}$. For each trial n and time point t with $p = p_n, s = s_n$, the embeddings determine the distribution over weights,

$$W_{n,t} \sim \mathcal{N}(\mu_n^w, \sigma_n^w), \quad \mu_n^w, \sigma_n^w \leftarrow \eta_{\theta}^w(z_p^p, z_s^s). \quad (9)$$

The likelihood model is now exactly the same as in TFA,

$$Y_{n,t} \sim \mathcal{N}(W_{n,t} \cdot F_p, \sigma^Y), \quad F_p \leftarrow \kappa(x_p^F, \rho_p^F), \quad (10)$$

We summarize the generative model for NTFA in Algorithm 1. This model defines a joint density $p(Y, W, x, \rho, z^p, z^s \mid \theta)$ and posterior distribution $p(W, x, \rho, z^p, z^s \mid Y, \theta)$ conditioned on Y . We approximate the posterior with a fully-factorized variational distribution,

$$q(W, \rho, x, z^p, z^s \mid \lambda) = \prod_{n,t} q(W_{n,t} \mid \lambda_{n,t}^w) \prod_s q(z_s \mid \lambda_s^s) \prod_p q(x_p^F \mid \lambda_p^x) q(\rho_p^F \mid \lambda_p^{\rho}) q(z_p \mid \lambda_p^p).$$

We learn the parameters θ and λ by maximizing the evidence lower bound (ELBO)

$$\mathcal{L}(\theta, \lambda) = \mathbb{E}_q \left[\log \frac{p(Y, W, x, \rho, z^p, z^s \mid \theta)}{q(W, x, \rho, z^p, z^s \mid \lambda)} \right] \leq \log p_{\theta}(Y).$$

To optimize this objective, we use Probabilistic Torch, a library for deep generative models that extends the PyTorch deep learning framework [Narayanaswamy et al., 2017]. This makes it comparatively straightforward to optimize objectives such as the evidence lower bound for general classes of user-defined models. We employ an importance-weighted objective [Burda et al., 2016] with a doubly-reparameterized gradient estimator [Tucker et al., 2019].

The advantage of incorporating neural networks into the generative model is that it enables us to explicitly reason about multimodal response distributions and effects that vary between individual samples. The network weights θ are shared across trials, as are the stimulus and participant embeddings z_s^s and z_p^p . This allows NTFA to capture statistical regularities within a whole experiment. At the same time, the use of neural networks ensures that differences in embeddings can be mapped onto a wide range of spatial and temporal responses. Whereas the hierarchical Gaussian priors in HTFA implicitly assume that response distributions are unimodal and uncorrelated across different factors k , the neural network in NTFA is able to model such correlations by jointly predicting all K factors.

While neural network models can have thousands or even millions of parameters, we emphasize that NTFA in fact has a *lower* number of trainable parameters than HTFA. TFA and HTFA assume fully-factorized variational distributions, requiring $O(NK + NTK)$ learned parameters for N trials

Algorithm 1 NeuralTFA Generative Model

(p_1, \dots, p_N)	▷ Participant for each trial
(s_1, \dots, s_N)	▷ Stimulus for each trial
1: for p in $1, \dots, P$ do	
2: $z_p^p \sim \mathcal{N}(0, I)$	▷ Equation (6)
3: for s in $1, \dots, S$ do	
4: $z_s^s \sim \mathcal{N}(0, I)$	▷ Equation (6)
5: for n in $1, \dots, N$ do	
6: $p, s \leftarrow p_n, s_n$	
7: $(\mu_p^x, \sigma_p^x), (\mu_p^\rho, \sigma_p^\rho) \leftarrow \eta_\theta^f(z_p^p)$	
8: $x_p^f \sim \mathcal{N}(\mu_p^x, \sigma_p^x)$	▷ Equation (7)
9: $\rho_p^f \sim \mathcal{N}(\mu_p^\rho, \sigma_p^\rho)$	▷ Equation (8)
10: $\mu_n^w, \sigma_n^w \leftarrow \eta_\theta^w(z_p^p, z_s^s)$	▷ Equation (9)
11: for t in $1 \dots T$ do	
12: $W_{n,t} \sim \mathcal{N}(\mu_n^w, \sigma_n^w)$	▷ Equation (9)
13: $F_p \leftarrow \kappa(x_p^f, \rho_p^f)$	
14: $Y_{n,t} \sim \mathcal{N}(W_{n,t} \cdot F_p, \sigma^Y)$	▷ Equation (10)

Table 1: **Number of learnable parameters:** When using low-dimensional embeddings, NTFA has roughly as many parameters as HTFA for the Pie Man dataset, and orders of magnitude fewer learnable parameters for other datasets, which have many more trials than participants ($N \gg P$).

Dataset	HTFA parameters $K = 100$	NTFA parameters $K = 100, D = 2$	HTFA log-likelihood	NTFA log-likelihood
Pieman	1.02×10^7	1.02×10^7	-5.22×10^9	-3.15×10^9
Depression	2.53×10^7	2.61×10^6	-1.22×10^9	-1.08×10^9
AffVids	1.64×10^8	8.88×10^6	-5.17×10^9	-3.87×10^9
Synthetic ($K = 3$)	2.16×10^4	1.90×10^4	-3.09×10^7	-2.19×10^7

with T time points. In NTFA, the networks η^f and η^w will have $O(DK)$ parameters each, whereas the variational distribution will have $O(D(P + S) + PK + NTK)$ parameters.

In practice, scanning time limitations impose a trade-off between N and T (the number of trials in a scanning run, and the length of a trial). For this reason NTK does not always dominate NK , since often $T \propto O(10)$. This means that we can obtain a lower-dimensional variational parameterization by choosing embedding dimensions D that are smaller than the number of factors K , and letting the neural networks model the $P \times S$ interaction between participants P and stimuli S . As summarized in Table 1, NTFA can have orders of magnitude fewer parameters when $D = 2$ as compared to HTFA.

4 Experiments

4.1 Datasets

We evaluate NTFA on four datasets, setting $D = 2$. First, we verify that NTFA can recover a ground-truth embedding structure that, by construction, contains clearly distinguishable participant and stimulus clusters. We then verify that NTFA can reconstruct the publicly available ‘‘Pie Man’’ dataset used to evaluate previous fMRI analysis models [Anderson et al., 2016]. We then present analysis on a publicly available dataset with more than one stimulus in each stimulus category, and finally on an in-house dataset, a pilot study pertaining to the subjective experience of fear. We present embedding results from these datasets analyzed without their resting-state trials. These experimental datasets vary in several qualities including the number of participants, time points, and voxels, and also task variables, testing how NTFA performs in a variety of experimental contexts.

Synthetic Data: To demonstrate that in addition to accurate reconstructions NTFA can also learn meaningful embeddings, we created a synthetic fMRI dataset. This dataset consists of three participant groups of five participants each, which we call *Group 1*, *Group 2* and *Group 3*. All participants underwent two categories of hypothetical stimuli, called *Baseline* and *Task*, with five stimuli within each category. Each participant underwent a single hypothetical scanning run with rest trials interleaved between stimuli. We manually defined three distinct factors in a standard MNI_152_8mm brain. We then sampled participant embeddings $\{z_1^p, \dots, z_{15}^p\}$ and stimulus embeddings $\{z_1^s, \dots, z_{10}^s\}$, from mixtures of three and two distinct Gaussians respectively (Figure 3). We set the means for these Gaussians so that when we noisily combined them, the following conditions would be met:

- All participants show no whole-brain response during rest besides random noise.
- Under *Baseline* stimuli, Group 1 exhibits half the response in the first region as compared to under *Task* stimuli, on average. The rest of the brain shows no response. Similarly, Group 2 and Group 3 exhibits a response in the second and third regions respectively, while the rest of the brain shows no response.
- Each *Baseline/Task* stimulus provokes a response lower or higher than the stimulus category’s average based on the location of the particular stimulus embedding.

“Pie Man” Narrative Listening [Simony et al., 2016]: In a between-subjects design, participants were assigned to one of four experimental stimulus categories that varied in the amount of structured narrative content that was presented. Participants either listened to an intact audio recording of a story ($N = 36$), or the same recording with paragraphs scrambled ($N = 18$) or with words scrambled ($N = 25$). A fourth group of participants were not presented with any recordings ($N = 36$). The fMRI data had 61,367 voxels and 300 time points for each scanning run. The narrative, entitled *Pie Man*, was presented at a story-telling event organized by *The Moth*. The full dataset is available online².

Emotional Musical and Nonmusical Stimuli in Depression [Lepping et al., 2016]: 19 participants with major depressive disorder, and 20 control participants ($N=39$) underwent emotional musical and nonmusical stimuli to examine how neural processing of emotionally provocative auditory stimuli is altered within the anterior cingulate cortex and striatum in depression. The fMRI data had 353,600 voxels, and 105 time points for each scanning run. The dataset is also available online³. We use the shorthand *Depression* to refer to this data.

The Fear and Affective Videos “AffVids” Dataset: This is a dataset for a pilot study that we have carried out in-house. A total of 22 participants watched videos depicting fear-related content and rated affective and emotional impact after each clip. The stimuli consisted of 36 videos, separated into three fear-related content situations (spiders, heights, and social situations), each clip lasting 20 seconds. Participants provided subjective experience ratings (e.g. how much fear they felt) after each clip. The fMRI data contained 81,638 voxels and 1656 time points per scanning run.

In addition to $D = 2$, we set $K = 100$ for analysis of the three real datasets.

4.2 Evaluation

We compare NTFA to HTFA in terms of its ability to reconstruct the data, before examining embeddings. For each dataset, we report the log-likelihood as a measure of reconstruction performance and the number of learned parameters to show model complexity.

Across datasets, NTFA exhibits a higher log-likelihood than HTFA, which is representative of the current state of the art (Table 1), with the same number ($K = 100$) of latent factors. Example reconstructions from the Depression and AffVids datasets are shown in Figure 2.

Synthetic Data: For synthetic data, NTFA recovers stimulus and participant embeddings that are qualitatively very similar to the embeddings that we used to generate the data (Figure 3). We emphasize that embeddings are learned directly from the synthetic data in an entirely unsupervised manner, which means that there is in principle no reason that we would expect embeddings to be exactly the same. However, we do observe that learned embeddings for participants and stimuli are well-separated, appear to have some variance, and are invariant under linear transformations.

²<http://arks.princeton.edu/ark:/88435/dsp015d86p269k>

³This data was obtained from the OpenfMRI database. Its accession number is ds000171.

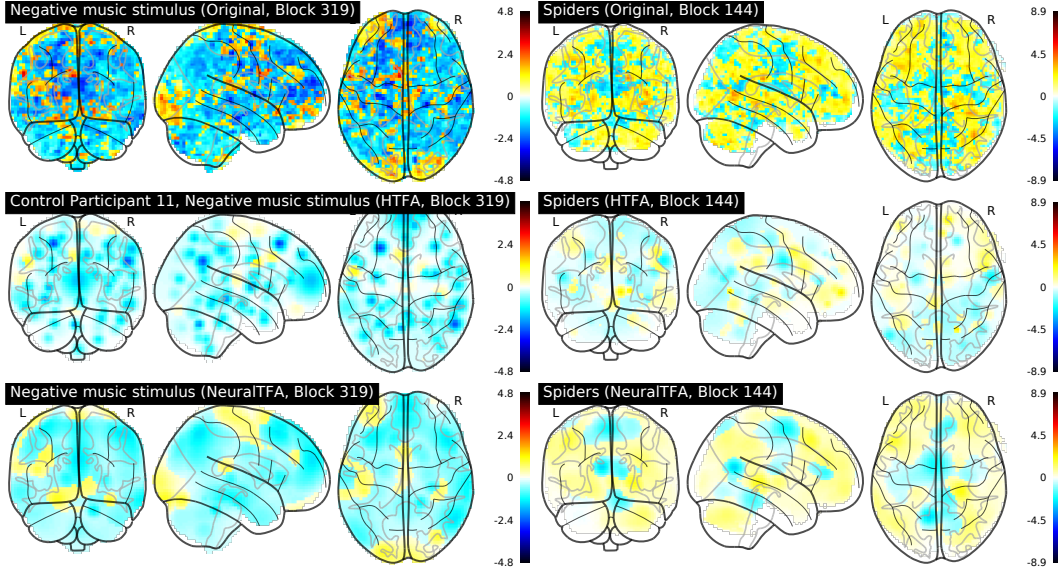


Figure 2: **Reconstructions for the Depression and AffVids datasets:** We show a sample brain scan (top) along with reconstructions from HTFA (middle) and NTFA (bottom). **Left:** NTFA (below) made more efficient use than HTFA (middle) of its parameter dimensionality at $K = 100$ to reconstruct the original image (above). **Right:** NTFA (below) more accurately captured complex spatial variations than HTFA (middle) in the original image (above).

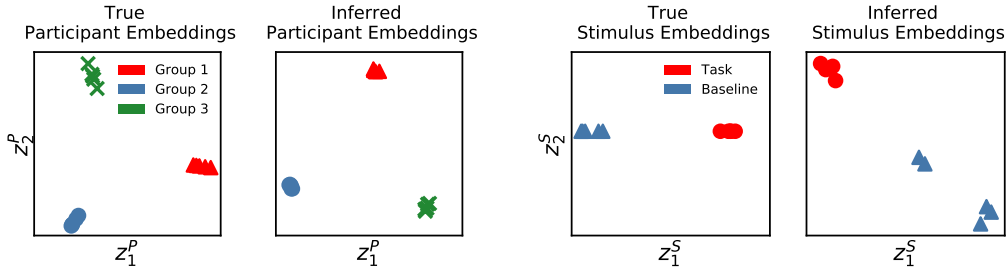


Figure 3: **Inferred embeddings for synthetic data:** We apply NTFA to a dataset in which three groups of participants exhibit varying levels of response in three different brain regions to *Task* and *Baseline* stimuli. NTFA, without prior knowledge of participant groups and stimulus categories, recovers these conditions as participant and stimulus embeddings, as shown in the “inferred” embeddings plots. Only the relative spatial arrangement is of interest, not exact positions in the embedding space.

Moreover, given the “true” number of factors ($K = 3$), NTFA is able to reconstruct synthetic data better than HTFA.

The “Pie Man” Narrative Listening dataset: The Pieman dataset [Simony et al., 2016] has previously been used to evaluate TFA and HTFA [Manning et al., 2018]. In this study, each participant underwent one trial with one stimulus in each scanning run, so only stimulus embeddings were shared across trials. This does not seem to have reduced NTFA’s reconstruction performance.

Emotional Musical and Nonmusical Stimuli in Depression dataset: On this dataset, NTFA similarly achieved better reconstruction performance than HTFA. An example reconstruction for this dataset can be seen in Figure 2. In analysis without resting-state data, stimulus embeddings display a gradation from tonal/musical to atonal/nonmusical, and participant embeddings show a gradation from control to major depressive participants (Figure 4). It is pertinent to mention that the labels in the figures are used for visualization purposes only; NTFA discovers this structure with no supervision.

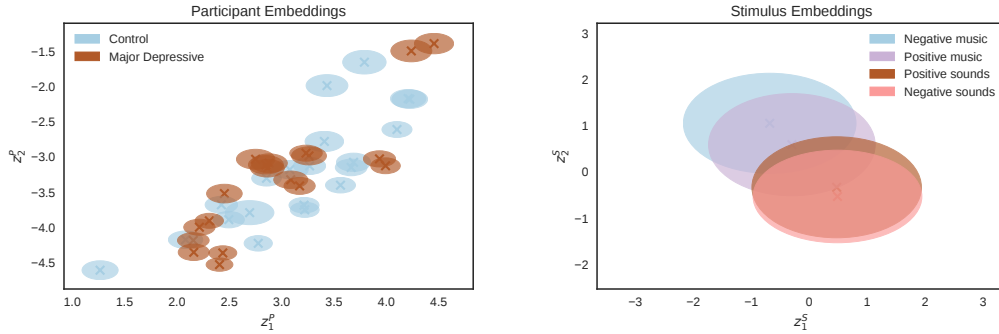


Figure 4: **Participant and stimulus embeddings from the Depression dataset [Lepping et al., 2016]:** NTFA learned participant and stimulus embeddings across groups and categories (respectively). Crosses indicate the location of the (approximate) posterior mean, and ellipses display (approximate) posterior covariance. **Left:** Participant embeddings spanned from mostly depressed (lower-left) to mostly control (upper-right) **Right:** Stimulus embeddings arranged stimuli from tonal (left) to atonal (right).

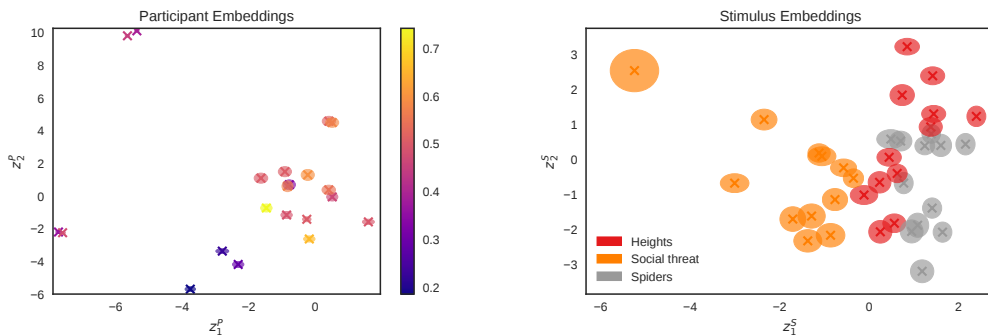


Figure 5: **Participant and stimulus embeddings from the AffVids dataset:** NTFA learned participant and stimulus embeddings meaningful for inferring behavioral measures and stimulus categories (respectively). Crosses indicate the location of the (approximate) posterior mean, and ellipses display (approximate) posterior covariance. **Left:** Participant embeddings arranged themselves into a cluster with greater self-reported fear across all stimuli, a smaller triad at the bottom reporting less fear across stimuli, and several outliers whose experience varies between stimuli. A lower value (cooler color) indicates a lower mean fear rating, while a higher value (warmer color) indicates a higher mean fear rating. **Right:** Stimulus embeddings recovered groups of fear stimuli corresponding to heights, spiders, and social threats. The overlap may reflect intentionally low fear intensity on the part of the stimulus designers, leading to decreased fear response and separability.

Fear and Affective Videos dataset: On the AffVids dataset from our in-house pilot study, NTFA achieves visibly better reconstructions than HTFA, as can be seen in Figure 2. In an analysis without resting-state data, NTFA uncovered stimulus embeddings that clustered by stimulus category (Figure 5). The participant embeddings uncovered a group more afraid across stimuli, a group less afraid across stimuli, and a group whose fear intensity varied between stimuli (Figure 5). Participants were not recruited in specific groups (e.g. arachnophobes and acrophobes), and stimuli could be categorized in multiple ways (e.g. by kind or degree).

5 Discussion

We have introduced Neural Topographic Factor Analysis (NTFA), an unsupervised model of spatio-temporal fMRI data which learns low-dimensional embeddings for participants and stimuli. We demonstrated that NTFA can recover ground-truth embedding clusters in synthetically generated data, and that it can reconstruct three datasets of real fMRI data better than the state-of-the-art using as few hidden factors as $K = 100$. NTFA attains higher log-likelihood than HTFA across data sets, for the same number of latent factors. When we set $D = 2$, NTFA learned embeddings from the real fMRI datasets that appeared to vary in a neuroscientifically meaningful way. This suggests that NTFA captures meaningful aspects of the underlying data.

Contrary to expectations of how a model can achieve superior reconstruction, we have seen that NTFA requires fewer parameters. In the case of the AffVids dataset, NTFA required on the order of 8.88 million parameters, as opposed to HTFA's 164 million parameters, two orders of magnitude of advantage in compressing and representing large datasets. This advantage is replicated in datasets with many more trials than participants ($N \gg P$), as shown in Table 1.

NTFA provides a path towards a more data-driven, discovery-oriented approach to investigating when neural activity varies across participants and stimuli, and when it remains relatively similar. Future work will be able to follow up on these initial findings by exploring how various parameter choices might improve sensitivity to such relationships.

Practically, these techniques reflect a growing and urgent need for scalable analysis approaches which can handle large datasets. That is, there are numerous nationwide and international efforts to collect large fMRI datasets of hundreds or thousands of participants performing numerous cognitive tasks. Traditional analyses which do not efficiently compress the underlying data are not suited to guide inferences performed across such large samples. The approach we describe here is ideally suited for such large datasets and might potentially be able to capture the meaningful aspects of the data in a way that is ultimately interpretable by clinicians and researchers alike.

Acknowledgments

The authors would like to thank Jeremy Manning for insightful conversations during his visit. This work was generously supported by Intel, startup funds from Northeastern University, the National Science Foundation (NCS 1835309), and the US Army Research Institute for the Behavioral and Social Sciences (ARI W911NF-16-1-0191).

References

- Hervé Abdi and Lynne J. Williams. Principal component analysis. *Wiley interdisciplinary reviews: computational statistics*, 2(4):433–459, 2010.
- Michael J. Anderson, Mihai Capota, Javier S. Turek, Xia Zhu, Theodore L. Willke, Yida Wang, Po Hsuan Chen, Jeremy R. Manning, Peter J. Ramadge, and Kenneth A. Norman. Enabling factor analysis on thousand-subject neuroimaging datasets. *Proceedings - 2016 IEEE International Conference on Big Data, Big Data 2016*, pages 1151–1160, 2016. doi: 10.1109/BigData.2016.7840719.
- Yuri Burda, Roger Grosse, and Ruslan Salakhutdinov. Importance Weighted Autoencoders. In *International Conference on Representations*, 2016.
- Samuel J Gershman, David M Blei, Francisco Pereira, and Kenneth A Norman. A topographic latent source model for fmri data. *NeuroImage*, 57(1):89–100, 2011.
- James V. Haxby, J. Swaroop Guntupalli, Andrew C. Connolly, Yaroslav O. Halchenko, Bryan R. Conroy, M. Ida Gobbini, Michael Hanke, and Peter J. Ramadge. A common, high-dimensional model of the representational space in human ventral temporal cortex. *Neuron*, 72(2):404–416, 2011.
- Aapo Hyvärinen, Juha Karhunen, and Erkki Oja. *Independent Component Analysis*. Wiley Online Library, 2001.
- Rebecca J. Lepping, Ruth Ann Atchley, Evangelia Chrysikou, Laura E. Martin, Alicia A. Clair, Rick E. Ingram, W. Kyle Simmons, and Cary R. Savage. Neural processing of emotional musical and nonmusical stimuli in depression. *PLOS ONE*, 11(6):1–23, 06 2016. doi: 10.1371/journal.pone.0156859. URL <https://doi.org/10.1371/journal.pone.0156859>.
- Jeremy R. Manning, Rajesh Ranganath, Waitsang Keung, Nicholas B. Turk-Browne, Jonathan D. Cohen, Kenneth A. Norman, and David M. Blei. Hierarchical topographic factor analysis. In *Pattern Recognition in Neuroimaging, 2014 International Workshop On*, pages 1–4. IEEE, 2014a.
- Jeremy R. Manning, Rajesh Ranganath, Kenneth A. Norman, and David M. Blei. Topographic Factor Analysis: A Bayesian Model for Inferring Brain Networks from Neural Data. *PLOS ONE*, 9(5): e94914, May 2014b. ISSN 1932-6203. doi: 10.1371/journal.pone.0094914.

- Jeremy R Manning, Xia Zhu, Theodore L Willke, Rajesh Ranganath, Kimberly Stachenfeld, Uri Hasson, David M Blei, and Kenneth A Norman. A probabilistic approach to discovering dynamic full-brain functional connectivity patterns. *NeuroImage*, 2018.
- Siddharth Narayanaswamy, T. Brooks Paige, Jan-Willem van de Meent, Alban Desmaison, Noah Goodman, Pushmeet Kohli, Frank Wood, and Philip Torr. Learning Disentangled Representations with Semi-Supervised Deep Generative Models. In I. Guyon, U. V. Luxburg, S. Bengio, H. Wallach, R. Fergus, S. Vishwanathan, and R. Garnett, editors, *Advances in Neural Information Processing Systems 30*, pages 5927–5937. Curran Associates, Inc., 2017.
- Rajesh Ranganath, Sean Gerrish, and David M Blei. Black Box Variational Inference. *Proceedings of the Seventeenth International Conference on Artificial Intelligence and Statistics*, 33:814–822, 2014. ISSN 15337928. URL <http://proceedings.mlr.press/v33/ranganath14.html>.
- Erez Simony, Christopher J Honey, Janice Chen, Olga Lositsky, Yaara Yeshurun, Ami Wiesel, and Uri Hasson. Dynamic reconfiguration of the default mode network during narrative comprehension. *Nature communications*, 7:12141, 2016.
- George Tucker, Dieterich Lawson, Shixiang Gu, and Chris J. Maddison. Doubly Reparameterized Gradient Estimators for Monte Carlo Objectives. In *International Conference on Learning Representations*, number 1, pages 1–12, 2019. URL <http://arxiv.org/abs/1810.04152>.